Quantum Electronics **30** (12) 1037 – 1042 (2000)

ACTIVE MEDIA

PACS numbers: 42.55.Vc; 52.50.Jm; 52.25.Nr
DOI: 10.1070/QE2000v030n12ABEH001861

Simulations of the kinetics of the active medium of an X-ray laser heated by high-power picosecond pulses

V Yu Politov, V A Lykov, M K Shinkarev

Abstract. The gain on the $3S-3P$ transitions of Ne-like ions produced upon material heating by high-power picosecond laser pulses was numerically simulated. The dependence of the gain on the average value of the nuclear charge Z and the irradiation intensity was investigated. The shortest wavelength of X-rays that can be produced from the plasma of Ne-like ions was predicted.

1. Introduction

The past decade saw the emergence of an interesting line of research in the field of collisionally pumped Ne- or Ni-like ion X-ray lasers (XRLs) involving picosecond laser pulses to produce the XRL active medium [1]. Experimentally confirmed numerical simulations [2] revealed a significant advantage of this method of forming the conditions for X-ray lasing.

When the plasma temperature T_e rises abruptly during $10^{-12}-10^{-11}$ s, the ground state of the working ions has no time to be depleted due to ionisation. At the same time, the pumping rate may rise proportionally to the temperature-dependent factor $\exp(-\varepsilon_u/T_e)/T_e^{1/2}$ (ε_u is the excitation energy of the upper level) up to the limiting one. These combined effects result in very high values of the population inversion and the gain K on the working transitions.

The calculations performed for some Ne-like ions with an average nuclear charge Z (Ti and Ge) [3, 4] showed that the maximum value of K on transitions with $\lambda_g \sim 300$, 200 Å amounts to 100 – 200 cm^{-1} in the region of critical plasma density, where the heating pulse is absorbed (the pulse duration was assumed to be 1 ps). If the refraction is neglected, a single-pass X-ray lasing in the mode of deep saturation becomes possible even for a small longitudinal size of the laser medium $L \sim 1$ cm. In this case, the commonly accepted criterion for the saturation threshold $KL \geqslant 15$ is satisfied with a nearly ten-fold safety margin.

It is evident that for such K, the collisional pumping of an X-ray laser can be efficient not only for medium-Z materials, but for those with a relatively high Z as well. This gives promise that employing picosecond lasers to produce XRL active media will allow one to obtain saturated X-ray emission in the short-wavelength spectral region down to the 'water window', i.e., to $\lambda_0 \sim 45$ Å (the radiation with $\lambda_g < \lambda_0$ is considered promising for biological research).

In this paper, we used numerical simulations to study the spatiotemporal dependence of the gain coefficients on the Ne-like ion transitions in materials different values of Z for different amplitudes of the picosecond pulse.

V Yu Politov, V A Lykov, M K Shinkarev Russian Federal Nuclear Centre, All-Russian Research Institute of Technical Physics, P.O.Box 245, 456770 Snezhinsk, Chelyabinsk oblast, Russia

Received 16 August 2000
Kvantovaya Elektronika **30** (12) 1037 – 1042 (2000)
Translated by E N Ragozin

2. Underlying assumptions

Our simulations involve the gas dynamics of a laser target, which expands under high-power optical irradiation, and the kinetics of the resulting plasma medium. In accordance with a standard experimental practice, the irradiation time-profiled pulse is focused in a line on a plane solid target. The initial extended and relatively low-intensity part of the pulse serves for forming the quasi-stationary ion composition of the plasma optimal for an X-ray laser, while its second part serves to rapidly heat the plasma.

The time shape of the irradiation pulse was represented in the form of a 1-ns long pedestal and a triangular high-intensity peak with a half-width $t_0 = 10$ ps (hereafter, the latter will be referred to as the picosecond pulse). The choice of t_0 was governed by the following considerations. For a finite velocity of light, a significant reduction in t_0 (down to ~ 1 ps) requires the use of the travelling-wave pumping of the XRL, which is an intricate technical problem. In addition, this will be accompanied by a reduction in the XRL output energy. An increase in t_0 is also undesirable, because the ion composition will begin to appreciably shift towards higher-charge (in comparison with Ne-like ions) ions, resulting in the decrease in K. The upper bound for the picosecond pulse duration can be estimated from the condition

$$t_0 \leqslant \frac{1}{j_{Ne}} \tag{1}$$

and the interpolation Lotz formula for the ionisation rate j_{Ne} of the ground Ne-like state [5]:

$$j_{Ne} = 6\times 10^{-8}\mathrm{Ry}^{3/2} m_0 \times \frac{N_e T_e^{1/2}}{\varepsilon_{Ne}^2(1+0.4T_e/\varepsilon_{Ne})}\exp\left(-\frac{\varepsilon_{Ne}}{T_e}\right). \tag{2}$$

Here,

$$N_e = 6\times 10^{23}\,\frac{\langle Z\rangle\rho}{A};$$

$\varepsilon_{Ne} = 0.25\text{Ry}(Z-6.6)^2$ is the ionisation potential of Ne-like ions; $m_0 = 8$ is the number of equivalent electrons; A is the atomic weight; ρ is the density of the plasma medium in g cm^{-3}; Ry = 0.0136 keV; $\langle Z \rangle$ is the number of free electrons per ion, or the average degree of ionisation; j_{Ne} is measured in s^{-1}; T_e and ε_{Ne} in keV; and N_e in cm^{-3}. For temperatures $T_e \approx 0.5\varepsilon_{Ne}$ desirable for efficient collisional pumping and a typical ratio $\langle Z \rangle / A \simeq 0.3$, from expressions (1) and (2) we obtain

$$t_0 \leqslant 1.5 \times 10^{-17} \frac{(Z-6.6)^3}{\rho}. \quad (3)$$

It follows from (3) that the duration t_0 of the picosecond pulse of the first harmonic of a Nd laser should not exceed $10^{-11} - 10^{-12}$ s for the $20 \leqslant Z \leqslant 50$ range and a density of the active medium close to the critical one ($\rho_{cr} \approx 0.006$ g cm^{-3}).

3. Results of gas dynamic simulations

The gas dynamics of the XRL active media was calculated employing the one-dimensional Lagrangian SS-9 code [6] developed at the All-Russian Research Institute of Experimental Physics (VNIIEF). The code implements the model of absorption due to the inverse bremsstrahlung of the driving pulse in plasma layers with $\rho \leqslant \rho_{cr}$; the contribution of effects responsible for the production of fast electrons is neglected as regards the energy balance of the plasma. The radiation transfer is treated in the spectral kinetic approximation with inclusion of the kinetics of nonequilibrium material ionisation.

As shown by our calculations, the so-called self-consistent mode of target expansion [7] is realised at the extended prepulse stage. In this case, a relatively long isothermal plasma corona is formed, which completely absorbs the laser radiation in the sub-critical region. The prepulse intensity I_{pr} was selected assuming that ground-state Ne-like ions prevail in the charge-state distribution in the corona (the greater number of these ions, the higher the rate of population of the upper laser levels). For the materials under consideration (from titanium to silver), $I_{pr} = 2 \times 10^{11} - 3 \times 10^{13}$ W cm^{-2}. The dependence of the ground-state population of Ne-like ions on I_{pr} is demonstrated for Ge and Ag in Fig. 1.

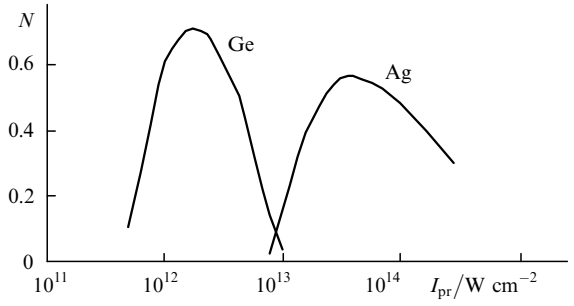

Figure 1. Calculated normalised populations of the ground state of Ne-like Ge and Ag ions in the critical-density region of a laser-produced plasma as functions of the prepulse intensity.

As for the density distribution in the corona, it is well approximated by the exponential dependence $\rho \approx \rho_{cr} \times \exp(-x/L_n)$, where x is the current coordinate in the direction normal to the target evaporation plane; L_n is the density gradient scale length, which ranges from 10 to 100 – 150 μm for the values of Z considered. The typical calculated density profiles are shown in Fig. 2. At the instant of prepulse completion, the density gradient scale length L_n and the corona temperature T_{e0} depend only on the average degree of ionisation $\langle Z \rangle$:

$$L_n \simeq 10^{-5}\langle Z \rangle^2, \quad T_{e0} \simeq 10^{-3}\langle Z \rangle^2; \quad (4)$$

for the prepulse intensity selected, $\langle Z \rangle \simeq Z - 11$.

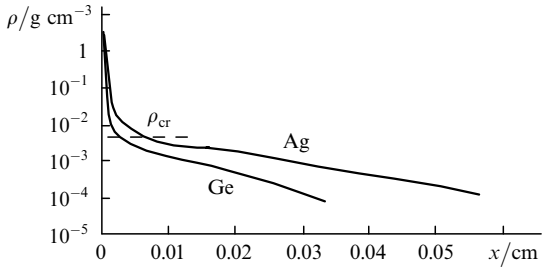

Figure 2. One-dimensional spatial density profiles of the plasma corona of Ge and Ag at the completion of the 1-ns prepulses with respective optimal intensities $I_{pr} = 2 \times 10^{12}$ and 3×10^{13} W cm^{-2} for $\lambda = 1.06$ μm.

At the stage of absorption of a high-power picosecond pulse, the plasma volume and density have no time to alter, and only a sharp increase in the electron temperature occurs, which favours X-ray lasing. Examples of the spatiotemporal distributions of Te for Ge and Ag at the completion of the picosecond pulse with a peak intensity $I_m = 10^{15}$ W cm^{-2} are given in Fig. 3. Due to a reduction in the absorption coefficient of laser radiation in the corona during its heating, the peaks of these distributions shift to the critical region and reach several kiloelectronvolts. Fig. 4 shows the corresponding dependences of the peak temperatures T_{em} on Z for the first and third harmonics of a Nd laser and different I_m.

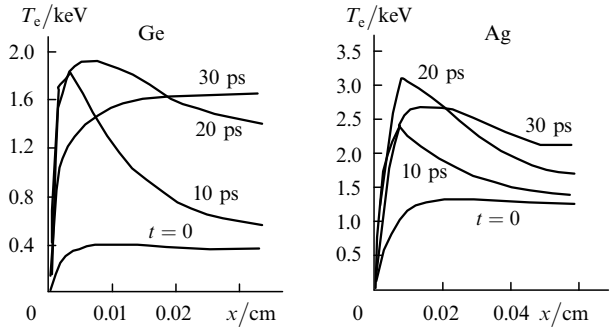

Figure 3. Spatial dependences of the electron temperature in the plasma corona of Ge and Ag at different point in time relative to the onset of a 10-ps pulse with a peak intensity of 10^{15} W cm^{-2} and $\lambda = 1.06$ μm.

These intensities can be analysed using the heat balance equation. According to this equation, the increase in T_e is limited by the electron thermal conduction, which transfers the absorbed laser energy to the dense cold plasma region with $\rho \geqslant \rho_{cr}$ (the energy losses of the plasma due to ionisation

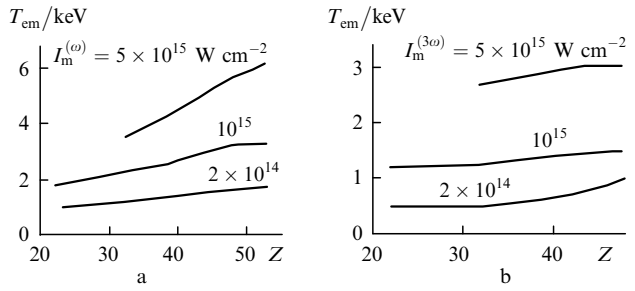

Figure 4. Values of the peak electron temperature of the plasma corona heated by a 10-ps pulse at the frequency of the first (a) and third (b) harmonic of a Nd laser calculated as functions of Z for three values of absorbed intensity.

and X-ray emission during the picosecond pulse can be neglected).

The fraction of energy that goes to heat the material in the supercritical region is rather difficult to estimate analytically, because the density distribution in it is highly nonuniform. In addition, for $I_m \geqslant 10^{15}$ W cm^{-2} the electron heat flux is limited at the front of the thermal wave, which complicates the functional relation between the heat flux and the temperature. More simple therefore is a consideration of the balance at the point with a density $\rho_* < \rho_{cr}$, where the major portion of the prepulse is absorbed and the role of heat transfer is not significant. For a self-consistent mode of the plasma corona expansion, this point is close to the so-called Jouguet point, at which the sound velocity coincides with that of gas-dynamic material motion. Subsequent heating of the nearest region by a high-power picosecond pulse causes T_e to rise up to values comparable to T_{em}.

The equation for the temperature of an ideal electron plasma at the Jouguet point, neglecting of the thermal conduction, is obtained by integrating the initial balance equation over the corona region with $0 \leqslant \rho \leqslant \rho_*$:

$$\frac{3}{2} N_A \frac{\langle Z \rangle \rho_* L_n}{A} \frac{\partial T_e}{\partial t} = I(t)\left[1 - \exp\left(-L_n \int_0^{\rho_*} d\rho \frac{k_b(\rho, T_e)}{\rho}\right)\right], \quad (5)$$

where $I(t)$ is the time profile of the laser pulse intensity; k_b is the absorption coefficient due to inverse bremsstrahlung in cm^{-1}; and N_A is the number of ions. For subcritical densities, the commonly accepted expression for k_b (see, e.g., Ref. [8]), taking into account (2), can be written in the form

$$k_b = \frac{4\sqrt{2}}{3\sqrt{\pi}} \frac{\langle Z \rangle e^6 N_e^2 \lambda^2}{(m_e T_e)^{3/2} c^3} \ln \Lambda \approx 10^6 \frac{\langle Z \rangle \rho^2 \lambda^2}{T_e^{3/2}}. \quad (6)$$

In this case, the temperature should be measured in keV, the laser radiation wavelength in micrometers, the Coulomb logarithm should be taken as $\ln \Lambda \approx 10$, and $\langle Z \rangle / A \approx 0.3$.

By definition of the point with $\rho = \rho_*$, the exponent in expression (5) at the onset of the picosecond pulse should be equal to unity; then, it will only decrease. This permits the exponent to be expanded in a series with retention of the terms no higher than the first-order term; after integration with respect to ρ, we obtain

$$\frac{\partial T_e^{5/2}}{\partial t} = 0.026 I(t) \langle Z \rangle \rho_* \lambda^2. \quad (7)$$

The density ρ_* is found from the condition that the absorbed prepulse energy be maximum, which is written as $L_n k_b(\rho_*, T_{e0}) = 2$. From this expression it follows, taking into account (4), that

$$\rho_* \approx \frac{2.5 \times 10^{-3}}{\lambda}. \quad (8)$$

The solution of Eqn (7), assuming that $T_{em} \gg T_{e0}$ and taking into account (8), yields the peak temperature as a function of I_m, t_0, λ, and $\langle Z \rangle$:

$$T_{em} \approx \left(6.5 \times 10^9 t_0\right)^{2/5} \left(I_m \times 10^{-14} \langle Z \rangle \lambda\right)^{2/5}. \quad (9)$$

For the accepted pulse duration $t_0 = 10^{-11}$ s, the values of T_{em} obtained using this formula agree reasonably well (to within 10 – 30 %) with the calculated ones.

4. Amplification characteristics of the XRL

The gain K for a plasma of Ne-like ions was determined using the TARAN code [9] for the calculation of level kinetics. This code uses the spatiotemporal distributions of the density $[\rho(x,t)]$ as well as the electron $[T_e(x,t)]$ and ion $[T_i(x,t)]$ temperatures obtained in gas-dynamic calculations, to solve the system of transient kinetic equations for the populations of discrete ion states in terms of which the gains K on the laser transitions are expressed. The system of equations is solved employing the Lagrangian cells corresponding to a one-dimensional spatial network $x(t)$.

The kinetic model incorporated in the code takes into account all the most significant collisional-radiative processes in the plasma: spontaneous radiative decay, collisional excitation and deexcitation, collisional, photo-, and dielectronic recombination, and also the corresponding inverse processes of ionisation. The plasma opacity in resonance lines is described in the approximation of photon escape from a medium without absorption (the Biberman – Holstein approximation). It is assumed that the lines have Voigt profiles. In the case of plane expansion, the dynamic Doppler effect is also included.

To form the kinetic matrix for the specific problem, we developed a problem-oriented database containing the spectroscopic description of different ionic states and transitions between them as well as the algorithm for retrieving these data. The basic spectroscopic information is the ionisation potentials, the statistical weights, the line strengths, the collision cross sections, etc. As for the degree of detailing of the energy spectra of the ions, the states are subdivided into the so-called unsplit and split ones. The former are characterised only by the principal quantum number n of the excited optical electron and the core configuration. The latter are described employing the sets of all quantum numbers, including the total ion momenta J. The unsplit states are described for all Z with $n \leqslant 10$ – from bare nuclei to neutrals. As for the states of the fine structure, by now the comprehensive data have been systematised for five ion species: H-, He-, Ne-like ions with $n \leqslant 4$ and Li-, Na-like ions with $n \leqslant 5$.

In the simulations of the kinetics of collisional XRL pumping, account was taken of a maximum of 89 states of Ne-like ions split in J with $n = 2$, 3, and 4. Certain of the results of kinetic simulations are given in Figs 5 and 6. First of all, these are the spatial distributions of the gain coefficient

on the strongest laser transition from the $3S-3P$ multiplet for Ge and Ag irradiated by the first harmonic of a Nd laser. (Depending on Z, this transition is either $2\bar{P}_{1/2}3P_{1/2}(0)-2\bar{P}_{1/2}3S_{1/2}(1)$ or $2\bar{P}_{3/2}3P_{1/2}(0)-2\bar{P}_{3/2}3S_{1/2}(1)$; for $Z<30$, some $3P-3D$ transitions inverted due to reabsorption on the $2P-3D$ transition also have comparable strengths [4].) They take place for about 10–20 ps after the peak of the picosecond pulse. In the medium-Z region, this time is enough to realise the quasi-stationary mode of saturated X-ray lasing. For relatively high Z, it may be that the lowering of K will generate the need to organise the travelling-wave pumping of an XRL active medium.

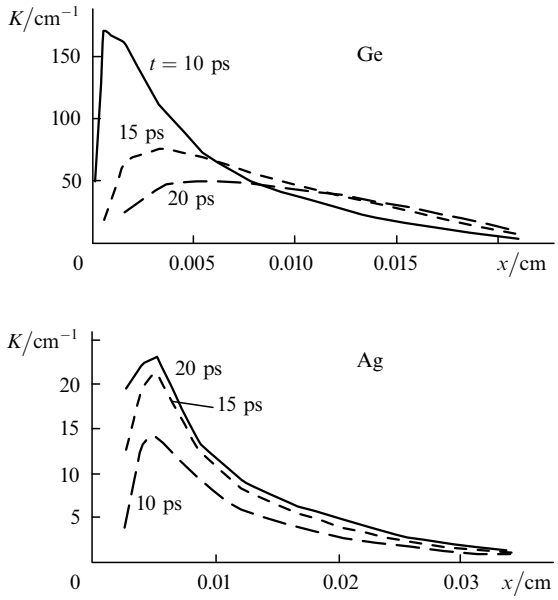

Figure 5. Spatial profiles of gains calculated for the strongest $3S-3P$ transition for Ge and Ag for $I_m = 10^{15}$ W cm^{-2} for several points in time relative to the onset of the picosecond pulse.

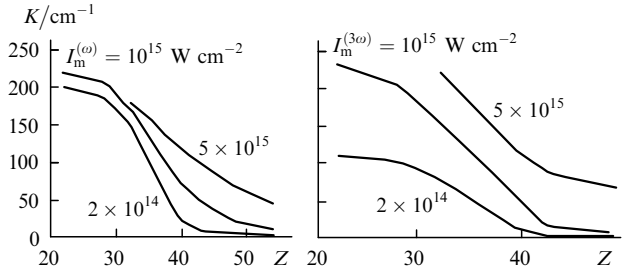

Figure 6. Peak gains on the $3S-3P$ transitions of Ne-like ions calculated for different-Z materials for three values of absorbed intensity of the first and third Nd-laser harmonic.

The distributions of this kind allowed us to construct the dependences of the maximum values of K_m on Z (Fig. 6), which demonstrate the ultimate amplification capabilities of Ne-like ion plasmas. However, the lasing wave will develop with significantly lower increments. The point is that the X-rays propagating in the inhomogeneous corona of a laser-produced plasma experience refraction and escape the highest-gain region. Moreover, the finiteness of the velocity of light shows up (it travels a distance of 1 cm in about 30 ps, which is comparable with the inversion lifetime specified above).

The effective gain coefficient is determined by calculating the output XRL energy for different lengths of the active medium whereby the mode of strong saturation does not yet set in. In this case, the intensity of lasing builds up nearly exponentially with L and has only an insignificant back action on the spatiotemporal distributions of K. Clearly the bulk of the radiation is transferred by the beams whose curved trajectories are tangent to the narrow region with $K \sim K_m$ near the evaporation plane. On traversing a distance L along the target, each of them is deflected in the direction of the normal by some distance x_0, which is, as a rule, far shorter than L. In the geometrical optics approximation, the departure is proportional to the density gradient $\partial\rho/\partial x$ in the corona and the square of the displacement of the beam axis [10]. Then, the equation for the ray trajectory is of the following form:

$$x(y) \approx \frac{\lambda_g^2}{4\lambda^2}\frac{[y-L'(x_0)]^2}{L_n}\exp\left(-\frac{x(y)}{L_n}\right),\ x(L)=x_0, \quad (10)$$

where $0 \leqslant y \leqslant L$; $L'(x_0)$ is the coordinate of the turning point of the trajectory in the highest-gain region determined by x_0 (it is assumed that the departure $x=0$ at the point $y=L'$).

Accordingly, the output energy per unit solid angle is estimated by integrating the intensity with respect to the time and the coordinates of the point of exit of the rays from the laser corona:

$$E_g = \int_0^{x_m} dx_0 \int_0^{\infty} dt I_{ray}(x_0, t), \quad (11)$$

where x_m corresponds to the ray with $L'=0$. The formal solution of the transport equation along each curved ray with accounting for the radiation propagation delay and the condition $x_0 \ll L$ can be written as

$$I_{ray} = \int_0^L dy I_s\left[x(y), t-\frac{L-y}{c}\right] \times \exp\left\{\int_y^L dy' K\left[x(y'), t-\frac{L-y'}{c}\right]\right\}, \quad (12)$$

where I_s is the intensity of spontaneous radiation and c is the velocity of light. From the calculations of kinetics it follows that the population density of the upper laser level far exceeds that of the lower laser level for a fast picosecond pumping. As a consequence, I_s and K as functions of the spatial coordinates are close to each other, permitting the ray intensities to be expressed in terms of only the known values of the gain:

$$I_{ray} \sim \exp\left\{\int_y^L dy K\left[x(y), t-\frac{L-y}{c}\right]\right\} - 1. \quad (13)$$

Numerical integration of expression (11) gives, in view of expression (13) and specific beam trajectories according to Eqn (10), the required energy E_g as a function of L. For Ge, this dependence corresponds to an effective growth increment $K_{eff} \sim 50$ cm^{-1} (Fig. 7) for $K_m \sim 150$ cm^{-1}. For Ag with a significantly more extended corona and a smoother density distribution, $K_{eff} \sim 15$ cm^{-1}, which is little less than the peak value of ~ 20 cm^{-1}.

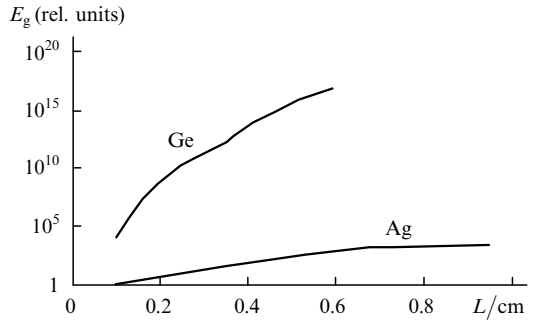

Figure 7. XRL radiation intensity as a function of the length of the laser target with the inclusion of refraction and radiation delay for Ge ($K_{\text{eff}} \sim 50$ cm^{-1}) and Ag ($K_{\text{eff}} \sim 15$ cm^{-1}).

The final result of the simulation cycle is the laser wavelength λ_g attainable in the saturation mode, which is calculated as a function of the amplitude of the driving picosecond pulse (Fig. 8). Orienting ourselves to laser target lengths $L \sim 1$ cm, we adopted the condition $K_{\text{eff}} \geqslant 15$ cm^{-1} as the saturation criterion. This dependence suggests that generating the saturated XRL radiation with $Z \geqslant 50$ and $\lambda_g < 70$ Å is possible only for absorbed laser intensities no lower than $(3-5) \times 10^{15}$ W cm^{-2}. The total irradiation energy is estimated at about a kilojoule, considering that the efficiency of conversion of the initial picosecond pulse to the energy of thermal electrons due to inverse bremsstrahlung is different from unity (estimates suggest that it is no greater than 50% for the calculated temperatures and gradient scale lengths). So high an energy is attainable with only the NOVA-type laser facilities. Mastering the 'water window' range in λ_g with the $3S-3P$ transitions of Ne-like ions is therefore extremely complicated today.

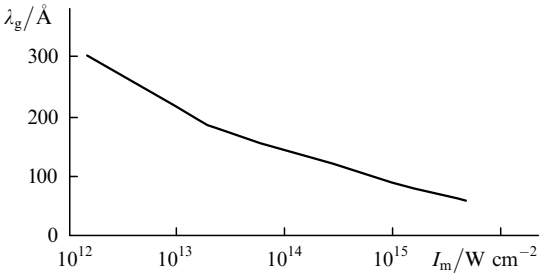

Figure 8. Wavelength of XRL radiation, for which a gain of over 15 cm^{-1} on Ne-like ions can be obtained, as a function of the picosecond pulse intensity.

There exists, however, an interesting possibility to obtain significantly harder X-ray radiation arising from the $2S-2P$ transitions of the same ions [11], with the population inversion produced owing to a strong monopole $2S-3S$ excitation. For Ar^{37+}, for instance, the $2\bar{S}_{1/2}3S_{1/2}(0) - 2\bar{P}_{3/2}3S_{1/2}(1)$ transition corresponds to $\lambda_g = 27$ Å. However, kinetic calculations suggest that the peak gain coefficients on these transitions do not exceed $3-5$ cm^{-1} for any pumping mode and arbitrary Z owing to significantly smaller values of the population inversion and oscillator strengths. The picosecond pumping of Ni-like ion plasmas with the $4P-4D$ working transitions is likely to offer greater promise as a way to reduce λ_g.

We also note that increasing the frequency of irradiation photons (going from the first Nd-laser harmonic to the third one) does not result in the increase of peak gain coefficients in Ne-like ion plasmas. Naturally, a harder radiation heats higher-density regions of the plasma corona, but the peak temperatures decrease in this case, which is crucial for collisionally pumped XRLs.

5. Conclusions

The results of the series of calculations outlined above demonstrate the amplification potentialities of Ne-like ions as functions of Z and the parameters of high-power optical pulses that produce the plasma XRL active medium. For materials with $Z \sim 20-30$ exposed to picosecond heating, the peak gain coefficients can run into the hundreds of inverse centimetres. Taking into consideration the refraction and the delay of radiation, it is more realistic to expect $K_{\text{eff}} \sim 40-50$ cm^{-1} for irradiation intensities of $\sim 10^{14}-10^{15}$ W cm^{-2}. These gain coefficients indicate that X-ray lasing with targets ~ 1 cm in length is possible in the deep-saturation mode, which has already been proved experimentally by the example of Ne-like titanium [12].

With increasing Z of the active medium of an XRL, the requirements on the irradiation intensity rise steeply. According to calculations, the generation of saturated XRL radiation with $Z > 50$ is possible only for $I_m \geqslant (3-5) \times 10^{15}$ W cm^{-2}, which necessarily implies the use of a picosecond pulse with $t_0 \geqslant 10^{-11}$ s and an energy of several kilojoules for the XRL pumping. This is primarily due to the fact that the maximum attainable temperatures in the corona of a laser-produced plasma, which determine the pumping efficiency, depends only relatively weakly on the picosecond pulse intensity $T_{\text{em}} \sim I_m^{2/5}$. This is so because a considerable portion of the irradiation energy is wasted by heating the dense and cold supercritical region of the corona.

Preparing the laser targets in the form of thin foils can increase the energy utilisation efficiency and hence alleviate attaining the 'water window' with Ne-like ion transitions. The role of electron thermal conduction will be diminished when such a target is completely turned into a plasma at the prepulse stage. A similar reduction of thermal losses is also possible when the prepulse wavelength is several times shorter than that of the main picosecond pulse (under these conditions, the density of the region supercritical for the main pulse is lowered).

References

1. Afanas'ev Yu V, Shlyaptsev V N *Kvantovaya Elektron.* **16** 2499 (1989) [*Sov. J. Quantum Electron.* **19** 1606 (1989)]
2. Nickles P V, Shlyaptsev V N, Schnuerer M, et al. *X-ray Lasers 1996 (Proceedings of the Fifth International Conference on X-ray Lasers, Lund, Sweden, 1996)* S Svanberg, C-G Wahlstrom (Eds) (Bristol: IOP Publishing, 1996) p. 84
3. Healy S B, Janulewicz K A, Plowes J A, Pert G J *ibid.* p. 94
4. Nilsen J Preprint No. UCRL-JC-125418 (Livermore, USA: Lawrence Livermore National Laboratory, 1996)
5. Vainshtein L A, Shevelko V P *Struktura i Kharakteristiki Ionov v Goryachei Plazme* (Structure and Characteristics of Ions in Hot Plasmas) (Moscow: Nauka, 1986)
6. Voinov B A, Gasparyan P D, Kochubei Yu K, et al. *Vopr. At. Nauki Tekh. Ser. Teor. Prikl. Fiz.* **2** 65 (1993)
7. *The Physics of High Energy Densities* P Caldirola, H Knoepfel (Eds) (New York: Academic Press, 1971)

8. Zel'dovich Ya B, Raizer Yu P *Physics of Shock Waves and High-Temperature Hydrodynamic Phenomena* (New York: Academic Press, 1966, 1967) Vols 1 and 2
9. Politov V Yu, Lykov V A, Shinkarev M K, in *Proc. Laser–Plasma Interactions* (Shanghai, China, 1992) v. 1928
10. Lunney J G *Appl. Phys. Lett.* **48** 891 (1986)
11. Politov V Yu, Shinkarev M K *Pis'ma Zh. Eksp. Teor. Fiz.* **58** 794 (1993) [*JETP Lett.* **58** 740 (1993)]
12. Dunn J, Osterheld A L, Shepherd R L, et al. *Proc. SPIE Int. Soc. Opt. Eng.* **3156** 114 (1997)